Estimating bite force in extinct dinosaurs using phylogenetically predicted physiological cross-sectional areas of jaw adductor muscles (#73067)

First submission

Guidance from your Editor

Please submit by **12 May 2022** for the benefit of the authors (and your $200 publishing discount) .

Structure and Criteria
Please read the 'Structure and Criteria' page for general guidance.

Raw data check
Review the raw data.

Image check
Check that figures and images have not been inappropriately manipulated.

Privacy reminder: If uploading an annotated PDF, remove identifiable information to remain anonymous.

Files

Download and review all files from the materials page.

5 Figure file(s)
8 Table file(s)
2 Raw data file(s)

Structure and Criteria

Structure your review

The review form is divided into 5 sections. Please consider these when composing your review:

1. **BASIC REPORTING**
2. **EXPERIMENTAL DESIGN**
3. **VALIDITY OF THE FINDINGS**
4. General comments
5. Confidential notes to the editor

You can also annotate this PDF and upload it as part of your review

When ready submit online.

Editorial Criteria

Use these criteria points to structure your review. The full detailed editorial criteria is on your guidance page.

BASIC REPORTING

- Clear, unambiguous, professional English language used throughout.
- Intro & background to show context. Literature well referenced & relevant.
- Structure conforms to PeerJ standards, discipline norm, or improved for clarity.
- Figures are relevant, high quality, well labelled & described.
- Raw data supplied (see PeerJ policy).

EXPERIMENTAL DESIGN

- Original primary research within Scope of the journal.
- Research question well defined, relevant & meaningful. It is stated how the research fills an identified knowledge gap.
- Rigorous investigation performed to a high technical & ethical standard.
- Methods described with sufficient detail & information to replicate.

VALIDITY OF THE FINDINGS

- Impact and novelty not assessed. *Meaningful* replication encouraged where rationale & benefit to literature is clearly stated.
- All underlying data have been provided; they are robust, statistically sound, & controlled.
- Conclusions are well stated, linked to original research question & limited to supporting results.

Standout reviewing tips

The best reviewers use these techniques

Tip	*Example*
Support criticisms with evidence from the text or from other sources	*Smith et al (J of Methodology, 2005, V3, pp 123) have shown that the analysis you use in Lines 241-250 is not the most appropriate for this situation. Please explain why you used this method.*
Give specific suggestions on how to improve the manuscript	*Your introduction needs more detail. I suggest that you improve the description at lines 57- 86 to provide more justification for your study (specifically, you should expand upon the knowledge gap being filled).*
Comment on language and grammar issues	*The English language should be improved to ensure that an international audience can clearly understand your text. Some examples where the language could be improved include lines 23, 77, 121, 128 – the current phrasing makes comprehension difficult. I suggest you have a colleague who is proficient in English and familiar with the subject matter review your manuscript, or contact a professional editing service.*
Organize by importance of the issues, and number your points	*1. Your most important issue* *2. The next most important item* *3. …* *4. The least important points*
Please provide constructive criticism, and avoid personal opinions	*I thank you for providing the raw data, however your supplemental files need more descriptive metadata identifiers to be useful to future readers. Although your results are compelling, the data analysis should be improved in the following ways: AA, BB, CC*
Comment on strengths (as well as weaknesses) of the manuscript	*I commend the authors for their extensive data set, compiled over many years of detailed fieldwork. In addition, the manuscript is clearly written in professional, unambiguous language. If there is a weakness, it is in the statistical analysis (as I have noted above) which should be improved upon before Acceptance.*

Estimating bite force in extinct dinosaurs using phylogenetically predicted physiological cross-sectional areas of jaw adductor muscles

Manabu Sakamoto Corresp. 1

1 School of Life Sciences, University of Lincoln, Lincoln, United Kingdom

Corresponding Author: Manabu Sakamoto
Email address: msakamoto@lincoln.ac.uk

Biomechanical modelling is a crucial means to understand the biology and ecology of extinct species. However, key model parameters relating to the muscles, namely the physiological cross-sectional area (A_{Phys}) are often difficult to estimate from fossils where muscles are not preserved. Here, I present a Bayesian phylogenetic predictive modelling framework to generate posterior predictive distributions of A_{Phys} in extinct archosaurs from the relationship between A_{Phys} and a skull geometry predictor variable, skull width (W_{Sk}) given a phylogeny. Predicted A_{Phys} are reasonably accurate (up to 95%) given the known phylogenetic scaling relationship between the muscle parameter and predictor variable. Downstream biomechanical modelling yields bite force estimates that are in line with previous estimates based on muscle parameters from reconstructed muscles. Thus, phylogenetic predictive modelling provides a powerful means to predict soft tissue parameters for biomechanical modelling in extinct species from simple osteological predictor variables.

Estimating bite force in extinct dinosaurs using phylogenetically predicted physiological cross-sectional areas of jaw adductor muscles

Manabu Sakamoto[1]

[1]School of Life and Environmental Sciences, University of Lincoln, Lincoln, UK

msakamoto@lincoln.ac.uk

Key words

Bite force, dinosaurs, phylogenetic comparative methods, phylogenetic predictive modelling, physiological cross-sectional area, biomechanics

Abstract

Biomechanical modelling is a crucial means to understand the biology and ecology of extinct species. However, key model parameters relating to the muscles, namely the physiological cross-sectional area (A_{Phys}) are often difficult to estimate from fossils where muscles are not preserved. Here, I present a Bayesian phylogenetic predictive modelling framework to generate posterior predictive distributions of A_{Phys} in extinct archosaurs from the relationship between A_{Phys} and a skull geometry predictor variable, skull width (W_{Sk}) given a phylogeny. Predicted A_{Phys} are reasonably accurate (up to 95%) given the known phylogenetic scaling relationship between the muscle parameter and predictor variable. Downstream biomechanical modelling yields bite force estimates that are in line with previous estimates based on muscle parameters from reconstructed muscles. Thus, phylogenetic predictive modelling provides a powerful means to predict soft tissue parameters for biomechanical modelling in extinct species from simple osteological predictor variables.

Introduction

Biomechanical modelling is an important means to infer the functional performances, ecologies, and behaviours of extinct animals for which such features cannot be directly observed [1], e.g., in dinosaurs [2–6]. Biomechanical modelling can be particularly informative in terms of adaptive evolution and patterns of natural selection, when it outputs a single-value performance measure, such as bite force [7]. This is because performance measures like bite force represent tangible physical interactions with the environment in which the animals live or

lived in. Bite force has repeatedly been reported as being correlated with dietary ecology in extant species [8–12], and thus has been treated as being likely informative for extinct species.

As bite force is the output of a musculo-skeletal lever system [13], its estimation relies on input parameters derived from muscle anatomy and architecture, which is seldom preserved in fossils. Muscles thus need to be reconstructed first, then relevant muscle parameters estimated [2,5,6,14,15]. These parameters include the positions and orientations of muscle bodies, the weight of the muscle bodies, lengths of the muscle fibres, the pennation angles of muscle fibres, ~~and~~ the physiological cross-sectional area (A_{Phys}) of muscles. However, muscle parameters based on reconstructions are associated with some degree of uncertainty [5,16]. This owes to a number of reasons but chief among them is the unknowability of fibre lengths and pennation angles in fossil species, ~~but~~ these parameters vary substantially amongst living species and are generally poorly documented. Fibre lengths and pennation angles (but especially the former) are crucial architectural data in estimating A_{Phys}, which itself being the determining factor of bite force. This is because force is proportional to A_{Phys} [13] and thus the latter can be used to estimate muscle force using a known stress factor σ (commonly 0.3 N/mm^2).

Owing to difficulties and challenges facing muscle parameter reconstructions combined with the impact it has over downstream biomechanical modelling, there is need for a simple but reasonably accurate method of predicting A_{Phys} from skull geometries. Here, I present a Bayesian predictive modelling framework, the phylogenetic predictive model (PPM), to generate posterior predictive distributions of A_{Phys} from relationships between A_{Phys} and a skull geometry predictor variable, the skull width (W_{Sk}). Crucially, the aim of this paper is not to

present a method that accurately predicts A_{Phys} in fossil species from skull geometries, but a method that can predict A_{Phys} from skull geometries and phylogeny to the same level of accuracy as that measured from reconstructed muscles. Thus, the main objective is to provide the community with a tool to aid in reasonably accurate estimates of A_{Phys} in fossil organisms for which muscles are difficult to reconstruct.

Material and Methods

Functional Muscle Groups

Jaw adductor muscles in archosaurs are largely grouped and named based on developmental biology and various topological criteria such as their relative positioning to nerves and blood vessels [17]. However, from a functional perspective, the existing groupings are not necessarily congruent with lines of actions in a lever model. For instance, the *Musculus* (M) *pseudotemporalis superficialis* (mPSTs) is topographically and functionally similar to the *M. adductor mandibularis externus* (mAME) but are developmentally linked to the *M. pseudotemporalis profundus* (mPSTp), the latter of which is often physically connected to (and indistinguishable from) the *M. adductor posterior* (mAMP). This largely stems from the fact that the mPSTs and mAME both have cranial attachments in the temporal fossa, while the mPSTp and mAMP both attach onto the quadrate (Fig. 1). Thus, the mPSTs and mAME work together as inter-linked functional in-levers while the mPSTp and the mAMP work together as a separate set of inter-linked functional in-levers.

I distinguish three functional adductor groupings, largely following [2] and [4], and identified muscle body complexes as follows: 1) the temporal muscle group (mTemp),

consisting of mAME and mPSTs; 2) the quadrate muscle group (mQuad), consisting of the mPSTp and mAMP; and 3) the pterygoid muscle group (mPt), consisting of the M. pterygoideus (mPT). Practically, these approximate groupings are necessary as adductor muscles in smaller specimens are often difficult, if not impossible, to separate into the classic topological groupings, and as the goal of this study is to predict A_{Phys} in fossil species where we do not necessarily have detailed topological information. Furthermore, in the context of both biomechanical modelling and predictive modelling, approximation is often important in obtaining *accurate* predictions, which is not necessarily the most *precise* model.

Physiological Cross-Sectional Areas in Extant Species

A_{Phys} for extant species were calculated from muscle architecture data collected predominantly from literature but also from dissections [7] (*Struthio camelus*, one specimen; *Buteo buteo*, three specimens; *Larus fuscus*, two specimens; *Branta canadensis*, one specimen; *Gallus domesticus*, two specimens; Supplementary File "001-RawData--PCSA_Extant.xlsx"; specimens were collected by the Bristol Ornithological Club and were donated to the University of Bristol as part of a clinical veterinary anatomy lab practical, c. 2005-2006 [18]). A_{Phys} were calculated as:

$$A_{Phys} = (M\cos\theta) / (\rho L), \quad (1)$$

following [19], where M is the wet weight of the muscle body (g), θ is the mean pennation angle, ρ is the specific density (1.056×10-3 g/mm^3 [20]), and L (mm) is mean fiber length. In the case of parallel fibers θ is 0° and thus cosθ is 1.

Muscle measurements for A_{Phys} calculations were taken for two specimens of *Buteo buteo* and one specimen each of *Larus fuscus* and *Struthio camelus*. Muscles were weighed prior to sectioning to obtain M. Muscles were carefully sectioned under a microscope using a sharp scalpel. Incisions were made parallel to the length of the muscle fibers as much as possible. L and θ were measured using ImageJ [21]. For all specimens, fiber lengths were taken at multiple locations on one or more sections through each muscle, the mean of which was taken as L.

In some specimens, A_{Phys} were approximated using the gross cross-sectional area (A_{Gross}), as simply the cross-section taken perpendicular to the long axis of the muscle body [2]. A_{Gross} was measured in one specimen each of *S. camelus*, *B. buteo*, and *Branta canadensis*, and two specimens each of *L. fuscus*, and *Gallus gallus*. The muscle body was sectioned roughly perpendicular to the major axis of the muscle body, and its A_{Gross} was digitally measured using Image J. The mean value of the left and right sides was taken as the final A_{Gross} value. Comparisons reveal that measured A_{Gross} values are generally congruent with calculated A_{Phys} values [18].

Physiological Cross-Sectional Areas in Extinct Species

For extinct archosaurs, cross-sectional areas of the jaw adductor muscles were estimated as A_{Gross} using a variant of the dry skull method [22], whereby cranio-mandibular dimensions

(namely the areas of the supratemporal, subtemporal, and mandibular fenestrae) were used to bound the A_{Gross} of individual jaw adductor muscles. I measured A_{Gross} of the mAME, mPSTs, mPSTp+mAMP and mPT on photographs and diagrams of reconstructed skulls taken at various angles of view. These are conceptually similar to previously published methods to estimate A_{Gross} in extinct dinosaurs [2,15,23]. We further applied muscle pennation angle θ=45° for the mTemp group, θ=0° for the mQuad group, and θ=30° for the mPt group, based on average pennation angles in our extant archosaur samples. We applied the effects of pennation on to A_{Gross} through division of A_{Gross} by sinθ. This approximates A_{Phys} in fossil archosaurs.

Predictor variable

I used the width of the skull (W_{Sk}) as the predictor variable in the PPMs. W_{Sk} was chosen here as it has previously been demonstrated to predict bite force [11,24,25] and various jaw adductor muscles well. It is also readily available from the literature for a vast number of species for which muscle data do not exist, both extant and extinct. The utility of its wider applicability makes simple measures like W_{Sk} an ideal predictor in predictive modelling. W_{Sk} were mostly measured directly from osteological and fossil specimens where possible but augmented with data taken from photographs and literature.

Phylogeny

I used an informal supertree of saurians based on the Time Tree of Life (TTOL) [26] with fossil tips inserted manually at the appropriate phylogenetic locations [7] (Fig. 3). Divergence times for fossil branches are based on first appearance dates (FAD) with terminal tips extended to

144 their last appearance dates (LAD) using the paleotree R package [27]. I used the full range of
145 temporal durations to scale the branches, as this allows for the maximum amount of time
146 possible for trait evolution to occur [7]. Zero-length internal branch lengths were resolved by
147 sharing time with neighbouring branches using the "equal" method [27,28].
148

149 ## Phylogenetic Predictive Modelling

150 I used a Bayesian PPM [25,29] to predict A_{Phys} in extinct archosaurs. Separate PPMs were fitted
151 on each of the three muscle groups as outlined above with the relevant A_{Phys} as the response
152 variable and W_{Sk} as the predictor variable.

153 Model performance, or prediction accuracy, of each PPM was evaluated in a dataset
154 containing only the extant species (N=39) first, through Leave-One-Out Cross-Validation
155 (LOOCV). LOOCV procedure largely follows that outlined in [25], and is as follows: 1) the PPM
156 was first fit on the dataset leaving one species out (N-1) using Markov Chain Monte Carlo
157 (MCMC) generating a posterior distribution of predictive models; 2) the posterior predictive
158 models were used to predict A_{Phys} for the species that was left out from Step 1 based on the W_{Sk}
159 and phylogenetic position of that species; 3) the posterior distribution of predictions (posterior
160 predictive distribution) was evaluated against the actual A_{Phys} value recorded for that species. If
161 the observed value fell outside the vast majority of the posterior predictive distribution (i.e.,
162 beyond 95% of the distribution; $p_{MCMC} < 0.05$), then it is deemed that the actual A_{Phys} value is
163 significantly different from the posterior predictive distribution, meaning that the prediction
164 has failed in this particular species. I repeated these steps for all species in the data set (N=39)

and calculated the proportion of species for which the model succeeded in accurately predicting A_{Phys} out of the total sample size N.

I then predicted A_{Phys} for 53 fossil species of archosaurs (predominantly theropod dinosaurs). I first fitted a PPM on the N=39 dataset and generated a posterior distribution of predictive models. I then used the predictive models to generate posterior predictive distributions for all 53 fossil species using their W_{Sk} and phylogenetic positions. This procedure is largely identical to LOOCV but is conducted in one step instead of one species at a time [25]. For 20 of the 53 fossil species, A_{Phys} measured from reconstructed muscles exist, thus allowing for assessment of prediction accuracy in the abilities of the PPMs to predict A_{Phys} in fossil species.

Additionally, I evaluated prediction accuracy of PPMs on an expanded training set (N=59) that includes A_{Phys} for select fossil species (N=20) measured from reconstructed muscles [7] or taken from literature [3,5,6,30]. Prediction accuracy was evaluated through LOOCV as outlined above.

I then predicted A_{Phys} for the remaining 33 fossil species of dinosaurs (predominantly theropods). I first fitted a PPM on the N=59 dataset and generated a posterior distribution of predictive models. I then used the predictive models to generate posterior predictive distributions of A_{Phys} for all 33 fossil species using their W_{Sk} and phylogenetic positions.

All model fitting was conducted in BayesTraits V3 over three independent MCMC chains each. The chains were run for 35,000,000 iterations, with the first 25,000,000 iterations discarded as burn-in, and sampled every 10,000 iterations after convergence, to produce a posterior sample of 1,000 predictive models and associated parameters.

187

188 ## Bite Force Estimation

189 Using the predicted A_{Phys} I estimated bite force (F_{Bite}) for 30 of the 33 fossil dinosaur species for
190 which I predicted A_{Phys} through the PPM approach. I then compared those against F_{Bite}
191 estimated for the 19 of the 20 fossil archosaurs based on measured A_{Phys} reconstructions
192 included in the training set for the PPMs.

193 For each of the 30 fossil species for which I predicted A_{Phys}, I took the median value of
194 the posterior predictive distribution for each muscle. Muscle force (F_{Musc}) was then estimated
195 for each muscle as the product of A_{Phys} and tetanic stress σ at 0.3 N/mm^2 (or 300kPa). The
196 resulting F_{Musc} was then multiplied by the muscle moment arm to yield the torque of that
197 muscle. I measured relevant moment arms for each muscle following the procedures developed
198 in [4] (Fig. 4). Muscle moments were summed and divided by the distance between the fulcrum
199 (jaw joint) and bite point and multiplied by 2 to derive a bilateral F_{Bite}. F_{Bite} was estimated for
200 the anterior-most and posterior-most positions along the biting edge (tooth row or beak; Fig.
201 4).

202 F_{Bite} in fossil archosaurs were estimated in the same way as above but using A_{Phys}
203 measured from reconstructed muscles as outline in [7]. I compared F_{Bite} at the posterior-most
204 positions (maximum F_{Bite}) between the two sets of fossil species.

205

Results

Prediction accuracies of PPMs

Prediction accuracies of the PPMs in the initial training set consisting of only extant species (N=39) was at 87% for all three muscle groups. The prediction accuracies of the PPMs in predicting A_{Phys} for the 20 fossil species, as compared to their measured A_{Phys} were 25%, 45% and 35%, respectively for the mTemp, mQuad and mPt groups.

Prediction accuracies of the PPMs in the expanded training set including fossil species (N=59) were at 95%, 93% and 90% for the mTemp, mQuad and mPt groups, respectively. Out of the 20 fossil species included in the training set, in only two species (*Plateosaurus engelhardti* and *Herrerasaurus ischigualastensis*) did the PPMs fail to predict the observed A_{Phys}.

Bite Force Estimation

F_{Bite} estimated for the 30 fossil species based on predicted A_{Phys} are shown in Table 1. Compared to F_{Bite} estimated from reconstructed A_{Phys} in the 19 fossil species, these 30 F_{Bite} values fall along the expected relationship between F_{Bite} and W_{Sk} (Fig 5). Comparisons between closely related species of similar sizes reveal the accuracy in resulting F_{Bite} values: F_{Bite} for *Deinonychus antirhoppus* (predicted A_{Phys}) with W_{Sk} of 114.5mm is 706N, while F_{Bite} for *Dromaeosaurus albertensis* (reconstructed A_{Phys}) with W_{Sk} of 103mm is 885N; F_{Bite} for *Carnotaurus sastrei* (predicted A_{Phys}) with W_{Sk} of 300mm is 7,172N while F_{Bite} for *Majungasaurus crenatissimus* (reconstructed A_{Phys}) with W_{Sk} of 300mm is 7,845N.

Discussion

The analyses presented here largely demonstrates two interesting features of predicting A_{Phys} in extinct species. First, the addition of A_{Phys} values for extinct species (measured from reconstructed muscles) in the training set drastically improved prediction accuracy of extinct species: compare 25-45% prediction accuracy using the extant-only PPM with 90% prediction accuracy (18/20 species) using the PPM that includes fossil species. The most likely cause of this improvement is increased sample size, from N=39 to N=59. It is well known and demonstrated through simulations that evolutionary parameters, such as Pagel's λ [31] lose statistical power with smaller sample size, with a marked reduction at approximately N < 50 [32,33]. As the PPM approach taken here is also based on the Brownian motion model of phenotypic evolution, it has similar statistical properties to estimating λ, and would most likely encounter similar effects of sample size. Thus, increasing sample size to N=59, which is just above this threshold of N=50 previously suggested through both simulated [32] and empirical [33] cases, is likely the underlying cause for the improvement in prediction accuracy. Indeed, a similar recent study, which demonstrated that F_{Bite} estimated in extinct species are in line with those expected for animals of similar sizes, used a PPM based entirely on extant species but had a sample size of N = 188 [25].

It is also possible however that the act of including fossil estimates ~~in and of itself~~ does have some positive effect on improving prediction accuracy. It has been shown before that inclusion of extinct tips in phylogenetic comparative analyses preserved phylogenetic signal λ [31] in rates of phenotypic evolution deeper in the tree, while that of ultrametric trees degraded rapidly [33] – one interpretation is that subsequent evolution 'overwrote' signals

from deeper in the tree when only data from extant taxa are modelled, but including fossil data deeper in the tree adds this information into the model. Thus, data associated with extinct tips that are deeper in time likely improves parameter estimation in phylogenetic comparative models. The oldest species in my dataset are approximately 250 million years old and comparatively close in time to the root of the tree and may contribute to this type of effect on evolutionary parameter (e.g., Brownian variance) estimation and the resulting posterior distribution of predictive models.

Crucially, as A_{Phys} in dinosaurs are generally much larger than those in most of the extant species in this dataset (Fig 5), predicting for dinosaurs from PPMs based on the extant-only training set (N=39) is effectively extrapolating far beyond the range of the data.

A note of caution however is that low prediction accuracy of A_{Phys} in extinct species using the extant-only training set may also be indicative of uncertainties related to muscle reconstructions based on skull geometries [34]. However, high precision accuracy in the LOOCV of the N=59 training set indicate that variation within A_{Phys} from muscle reconstructions in extinct species are within expected range of variance given phylogeny and Brownian motion [25]. Crucially, the objective of this study is to develop a method to predict A_{Phys} in extinct species from skull geometries that are within the same range of accuracy as those measured from reconstructed muscles, not to accurately predict real in-life A_{Phys} values as a substitute of muscle reconstruction – i.e., this method is to augment gaps in muscle reconstructed A_{Phys} data. Increased prediction accuracy by expanding the training set (N=59) to include A_{Phys} estimates for 20 extinct species fulfils this purpose.

Second, the power of simple linear morphometrics (e.g., W_{Sk}) in predicting functionally important parameters is not to be taken lightly. The PPMs developed here are based only on W_{Sk} but is demonstrated to have prediction accuracy upwards of 95% depending on the muscle group. The fact that W_{Sk} is tightly correlated with F_{Bite} across multiple groups of vertebrates [24,25] is consistent with these results. W_{Sk} is also tightly linked with body size, often scaling isometrically, making it the ideal predictor in PPMs for its ability to ground the model to a theoretical scaling framework, e.g., expected scaling exponent between area and length. Simple metrics are also readily available across a wide taxonomic sample and can be collected from literature and osteological specimens, including fossils. PPMs based on such simple predictors are thus more versatile and robust.

Bite Force Estimates in Extinct Archosaurs

Using the A_{Phys} predicted from the PPMs, I estimated F_{Bite} in several extinct archosaurs. These values can be regarded as reasonably reliable estimates of true F_{Bite} in these extinct animals, given scaling relation with W_{Sk} and phylogeny. This owes to the fact that they are highly congruent with F_{Bite} estimates based on A_{Phys} measured from reconstructed muscles, which themselves have been demonstrated to be reasonably reliable estimates of F_{Bite} given size and phylogeny [25]. Thus, PPMs are a useful approach to expand on reliable F_{Bite} data based on simple metrics and phylogeny.

Discussion of F_{Bite} for individual species of interest are then valid and worth considering. Of note is that the large-bodied carnivorous dinosaurs, *Carcharodontosaurus saharicus* and *Acrocanthosaurus atokensis*, both reaching the size range of *Tyrannosaurus rex*, have F_{Bite} that

292 are substantially lower than the latter, at 16,984N and 25,449N respectively, compared to
293 48,505N of *T. rex*. *Carcharodontosaurus* is approximately the same size as *T. rex* but is here
294 shown to have had F_{Bite} that is approximately half of the latter. *Carcharodontosaurus* is typical
295 in build and skull proportion for a theropod dinosaur, so the fact that its F_{Bite} was only half of
296 that of *T. rex* is more likely a reflection of just how unique *T. rex* may have been compared to
297 other theropods of similar sizes. *Tyrannosaurus* had robust conical-shaped teeth and multiple
298 adaptations in the skull that allowed it to withstand immense forces [35]. Multiple lines of
299 evidence also point to habitual bone-crushing and -consumption in *T. rex* [5,36,37]. These
300 support the hypothesis that *T. rex* had at least a partial osteophagous diet, an ecology that was
301 likely different from other theropods.
302 A similarly, large-bodied carnivorous dinosaur, *Spinosaurus aegyptiacus*, is here
303 tentatively predicted to have had F_{Bite} at just under 12,000N, roughly in the same range as
304 *Sinraptor* (10,845N), *Gorgosaurus* (13,817N), and *Daspletosaurus* (16,641N), all substantially
305 smaller theropods. With the caveat that W_{Sk} for *Spinosaurus* was simply scaled up from the
306 skull-width ratio of *Suchomimus* [38], I offer additional support for this taxon to have had
307 unique feeding habits for a theropod of its size. *Spinosaurus* shows adaptations in the
308 craniomandibular morpho-functional complexes that are advantageous for generating relatively
309 faster shutting speeds with less muscle input force (higher displacement advantage) at the
310 expense of F_{Bite} (lower mechanical advantage) [4]. This would be congruent with a feeding
311 mode relying on fast-snapping jaws rather than slow crushing bites, which is commonly
312 observed in species with semi-aquatic feeding habits, including herons and egrets [39].
313

Conclusions

Here, I present a phylogenetic predictive modelling framework to predict soft tissue parameters (A_{Phys}) in extinct species from an osteological predictor variable (W_{Sk}). Predicted parameters are reasonably accurate given the known scaling relationship between the muscle parameter and predictor variable and phylogeny. Downstream biomechanical modelling yields performance metrics (F_{Bite}) that are in line with previous estimates based on muscle parameters from reconstructed muscles. Thus, phylogenetic predictive modelling provides a powerful means to predict soft tissue parameters for biomechanical modelling in extinct species from simple osteological predictor variables.

Acknowledgements

I would like to thank Chris Venditti for advice on phylogenetic comparative methods and building the phylogenetic predictive models and Andrew Meade for various technical support related to BayesTraits.

References

1. Anderson PSL, Bright JA, Gill PG, Palmer C, Rayfield EJ. 2012 Models in palaeontological functional analysis. *Biology Letters* **8**, 119–122. (doi:10.1098/rsbl.2011.0674)

2. Rayfield EJ, Norman DB, Horner CC, Horner JR, Smith PM, Thomason JJ, Upchurch P. 2001 Cranial design and function in a large theropod dinosaur. *Nature* **409**, 1033–1037.

3. Lautenschlager S. 2013 Cranial myology and bite force performance of Erlikosaurus andrewsi: a novel approach for digital muscle reconstructions. *Journal Of Anatomy* **222**, 260–272. (doi:10.1111/joa.12000)

4. Sakamoto M. 2010 Jaw biomechanics and the evolution of biting performance in theropod dinosaurs. *Proceedings of the Royal Society B: Biological Sciences* **277**, 3327–33.

5. Gignac PM, Erickson GM. 2017 The Biomechanics Behind Extreme Osteophagy in Tyrannosaurus rex. *Sci Rep-Uk* **7**, 2012. (doi:10.1038/s41598-017-02161-w)

6. Bates KT, Falkingham PL. 2012 Estimating maximum bite performance in *Tyrannosaurus rex* using multi-body dynamics. *Biology Letters* **8**, 660–664.

7. Sakamoto M, Ruta M, Venditti C. 2019 Extreme and rapid bursts of functional adaptations shape bite force in amniotes. *Proceedings of the Royal Society B: Biological Sciences* **286**, 20181932. (doi:10.1098/rspb.2018.1932)

8. Dumont ER, Davalos LM, Goldberg A, Santana SE, Rex K, Voigt CC. 2012 Morphological innovation, diversification and invasion of a new adaptive zone. *Proceedings Of The Royal Society B-Biological Sciences* **279**, 1797–1805. (doi:10.1098/rspb.2011.2005)

9. Santana SE, Dumont ER, Davis JL. 2010 Mechanics of bite force production and its relationship to diet in bats. *Functional Ecology* **24**, 776–784. (doi:10.1111/j.1365-2435.2010.01703.x)

10. Santana SE, Strait S, Dumont ER. 2011 The better to eat you with: functional correlates of tooth structure in bats. *Functional Ecology* **25**, 839–847. (doi:10.1111/j.1365-2435.2011.01832.x)

11. Herrel A, Podos J, Huber SK, Hendry AP. 2005 Bite performance and morphology in a population of Darwin's finches: implications for the evolution of beak shape. *Functional Ecology* **19**, 43–48.

12. Herrel A, Podos J, Vanhooydonck B, Hendry AP. 2009 Force-velocity trade-off in Darwin's finch jaw function: a biomechanical basis for ecological speciation? *Functional Ecology* **23**, 119–125. (doi:10.1111/j.1365-2435.2008.01494.x)

13. Sinclair AG, Alexander RM. 1987 Estimates of Forces Exerted by the Jaw Muscles of Some Reptiles. *Journal Of Zoology* **213**, 107–115.

14. Mazzetta GV, Cisilino AP, Blanco RE. 2004 Mandible stress distribution during the bite in Carnotaurus sastrei Bonaparte, 1985 (Theropoda : Abelisauridae). *Ameghiniana* **41**, 605–617.

15. Mazzetta GV, Cisilino AP, Blanco RE, Calvo N. 2009 Cranial Mechanics and Functional Interpretation of the Horned Carnivorous Dinosaur Carnotaurus Sastrei. *Journal Of Vertebrate Paleontology* **29**, 822--830.

16. Bates KT, Falkingham PL. 2018 The importance of muscle architecture in biomechanical reconstructions of extinct animals: a case study using Tyrannosaurus rex. *Journal Of Anatomy* **0**. (doi:10.1111/joa.12874)

17. Holliday CM, Witmer LM. 2007 Archosaur adductor chamber evolution: Integration of musculoskeletal and topological criteria in jaw muscle homology. *Journal Of Morphology* **268**, 457–484.

18. Sakamoto M. 2008 Bite force and the evolution of feeding function in birds, dinosaurs and cats. University of Bristol.

19. Sacks RD, Roy RR. 1982 Architecture of the Hindlimb Muscles of Cats - Functional-Significance. *Journal Of Morphology* **173**, 185–195.

20. Burkholder TJ, Fingado B, Baron S, Lieber RL. 1994 Relationship between Muscle-Fiber Types and Sizes and Muscle Architectural Properties in the Mouse Hindlimb. *Journal Of Morphology* **221**, 177–190.

21. Rasband WS. 2012 *ImageJ*. Bethesda, Maryland: U. S. National Institute of Health.

22. Thomason JJ. 1991 Cranial Strength in Relation to Estimated Biting Forces in Some Mammals. *Canadian Journal of Zoology-Revue Canadienne De Zoologie* **69**, 2326–2333.

23. Reichel M. 2010 A model for the bite mechanics in the herbivorous dinosaur Stegosaurus (Ornithischia, Stegosauridae). *Swiss Journal of Geosciences* **103**, 235–240. (doi:10.1007/s00015-010-0025-1)

24. Herrel A, Podos J, Huber SK, Hendry AP. 2005 Evolution of bite force in Darwin's finches: a key role for head width. *Journal Of Evolutionary Biology* **18**, 669–675.

25. Sakamoto M. 2021 Assessing bite force estimates in extinct mammals and archosaurs using phylogenetic predictions. *Palaeontology* **64**, 743–753. (doi:10.1111/pala.12567)

26. Kumar S, Stecher G, Suleski M, Hedges SB. 2017 TimeTree: A Resource for Timelines, Timetrees, and Divergence Times. *Mol Biol Evol* **34**, 1812–1819. (doi:10.1093/molbev/msx116)

27. Bapst DW. 2012 paleotree: an R package for paleontological and phylogenetic analyses of evolution. *Methods Ecol Evol* **3**, 803–807. (doi:10.1111/j.2041-210X.2012.00223.x)

28. Brusatte SL, Benton MJ, Ruta M, Lloyd GT. 2008 Superiority, competition, and opportunism in the evolutionary radiation of dinosaurs. *Science* **321**, 1485–1488. (doi:10.1126/science.1161833)

29. Organ CL, Shedlock AM, Meade A, Pagel M, Edwards SV. 2007 Origin of avian genome size and structure in non-avian dinosaurs. *Nature* **446**, 180–184. (doi:http://www.nature.com/nature/journal/v446/n7132/suppinfo/nature05621_S1.html)

30. Lautenschlager S, Brassey CA, Button DJ, Barrett PM. 2016 Decoupled form and function in disparate herbivorous dinosaur clades. *Sci Rep-Uk* **6**, 26495. (doi:10.1038/srep26495 https://www.nature.com/articles/srep26495#supplementary-information)

31. Pagel M. 1997 Inferring evolutionary processes from phylogenies. *Zoologica Scripta* **26**, 331–348. (doi:10.1111/j.1463-6409.1997.tb00423.x)

32. Freckleton RP, Harvey PH, Pagel M. 2002 Phylogenetic analysis and comparative data: A test and review of evidence. *American Naturalist* **160**, 712--726.

33. Sakamoto M, Venditti C. 2018 Phylogenetic non-independence in rates of trait evolution. *Biology Letters* **14**, 20180502. (doi:10.1098/rsbl.2018.0502)

34. Bates KT, Wang L, Dempsey M, Broyde S, Fagan MJ, Cox PG. In press. Back to the bones: do muscle area assessment techniques predict functional evolution across a macroevolutionary radiation? *Journal of The Royal Society Interface* **18**, 20210324. (doi:10.1098/rsif.2021.0324)

35. Cost IN, Middleton KM, Sellers KC, Echols MS, Witmer LM, Davis JL, Holliday CM. 2019 Palatal Biomechanics and Its Significance for Cranial Kinesis in Tyrannosaurus rex. *The Anatomical Record* **0**. (doi:10.1002/ar.24219)

36. Erickson GM, Olson KH. 1996 Bite marks attributable to Tyrannosaurus rex: Preliminary description and implications. *Journal Of Vertebrate Paleontology* **16**, 175–178.

37. Erickson GM, VanKirk SD, Su JT, Levenston ME, Caler WE, Carter DR. 1996 Bite-force estimation for Tyrannosaurus rex from tooth-marked bones. *Nature* **382**, 706–708.

38. Sereno PC *et al.* 1998 A long-snouted predatory dinosaur from Africa and the evolution of spinosaurids. *Science* **282**, 1298–1302.

39. Hone D, Holtz T. 2021 Evaluating the ecology of Spinosaurus: shoreline generalist or aquatic pursuit specialist? *Palaeontologia Electronica* **24**. (doi:10.26879/1110)

Figure 1

Jaw adductor muscles and functional muscle groupings in extant archosaurs.

A, attachment sites for jaw adductor muscles are identified on a skull of a herring gull (*Larus fuscus*). Abbreviations are as follows: mAME, M. adductor mandibulae externus; mPSTs, M. pseudotemporalis superficialis; mPSTp, M. pseudotemporalis profundus; mAMP, M. adductor mandibulae posterior; and mPT, M. pterygoideus. Adductor muscles are then depicted: B, all adductor muscles; C, temporal muscle group (mAME + mPSTs) only; D, the quadrate muscle group (mPSTp + mAMP) only; and the pterygoid muscle group (mPT) only.

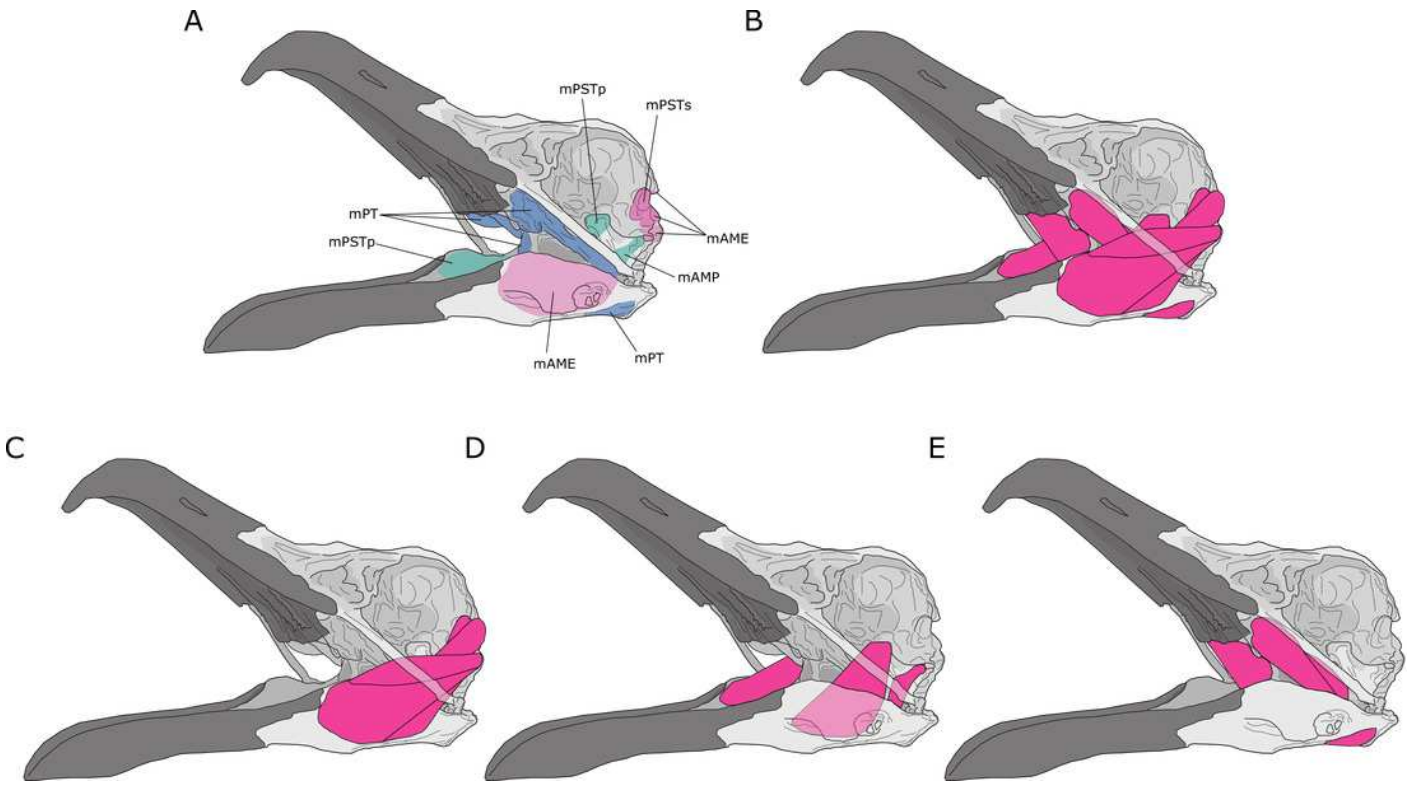

Figure 2

Relationships between physiological cross-sectional areas and skull width.

Relationships between physiological cross-sectional areas A_{Phys} for each of the three muscle groups and skull width (W_{Sk}) are shown for extant (blue) and extinct (red) archosaurs: A, temporal muscle group (mTemp); B, quadrate muscle group (mQuad); and C, pterygoid muscle group (mPt).

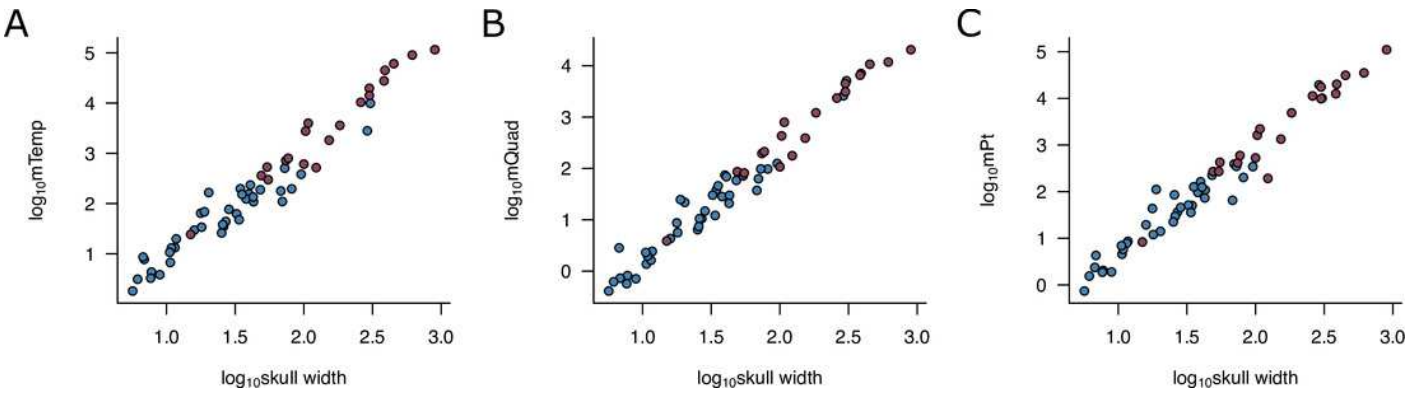

Figure 3

Phylogeny of extant and extinct saurians (N=59) used in the phylogenetic predictive modelling.

The extant portion of the tree was taken from the TimeTree of Life and extinct tips inserted at the relevant positions.

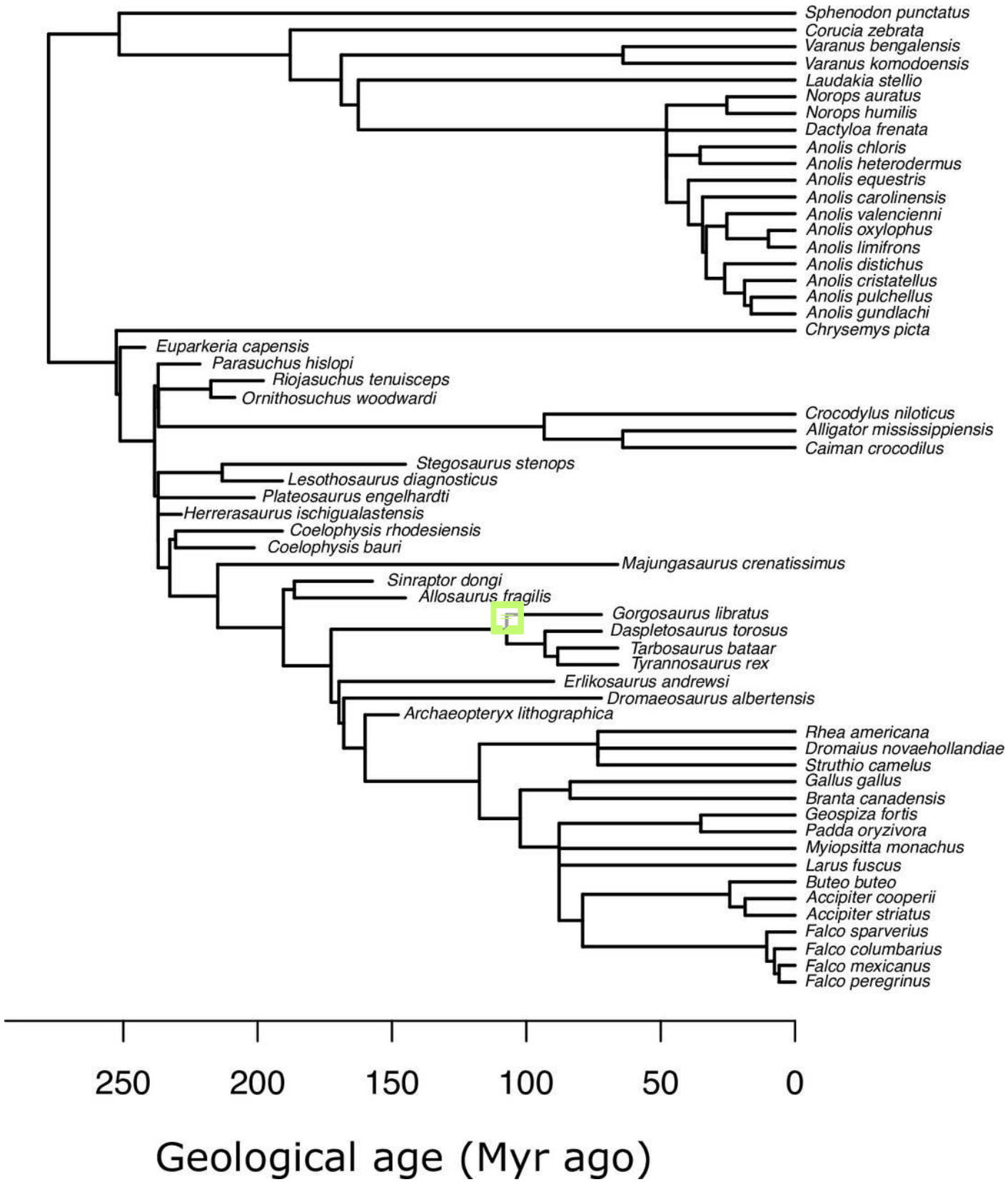
Sphenodon punctatus
Corucia zebrata
Varanus bengalensis
Varanus komodoensis
Laudakia stellio
Norops auratus
Norops humilis
Dactyloa frenata
Anolis chloris
Anolis heterodermus
Anolis equestris
Anolis carolinensis
Anolis valencienni
Anolis oxylophus
Anolis limifrons
Anolis distichus
Anolis cristatellus
Anolis pulchellus
Anolis gundlachi
Chrysemys picta
Euparkeria capensis
Parasuchus hislopi
Riojasuchus tenuisceps
Ornithosuchus woodwardi
Crocodylus niloticus
Alligator mississippiensis
Caiman crocodilus
Stegosaurus stenops
Lesothosaurus diagnosticus
Plateosaurus engelhardti
Herrerasaurus ischigualastensis
Coelophysis rhodesiensis
Coelophysis bauri
Majungasaurus crenatissimus
Sinraptor dongi
Allosaurus fragilis
Gorgosaurus libratus
Daspletosaurus torosus
Tarbosaurus bataar
Tyrannosaurus rex
Erlikosaurus andrewsi
Dromaeosaurus albertensis
Archaeopteryx lithographica
Rhea americana
Dromaius novaehollandiae
Struthio camelus
Gallus gallus
Branta canadensis
Geospiza fortis
Padda oryzivora
Myiopsitta monachus
Larus fuscus
Buteo buteo
Accipiter cooperii
Accipiter striatus
Falco sparverius
Falco columbarius
Falco mexicanus
Falco peregrinus
250
200
150
100
50
0
Geological age (Myr ago)

Figure 4

Static lever model to estimate bite force in extinct dinosaurs.

Bite force (F_{BAnt} and F_{BPost}) was estimated in extinct dinosaurs using a static lever model as shown on a skull and mandible reconstruction of *Deinonychus* (author's own work). F_{BAnt}, anterior bite force; F_{BPost}, posterior bite force; F_{Temp}, temporal group muscle force; F_{Quad}, quadrate group muscle force; F_{Pt}, pterygoid group muscle force.

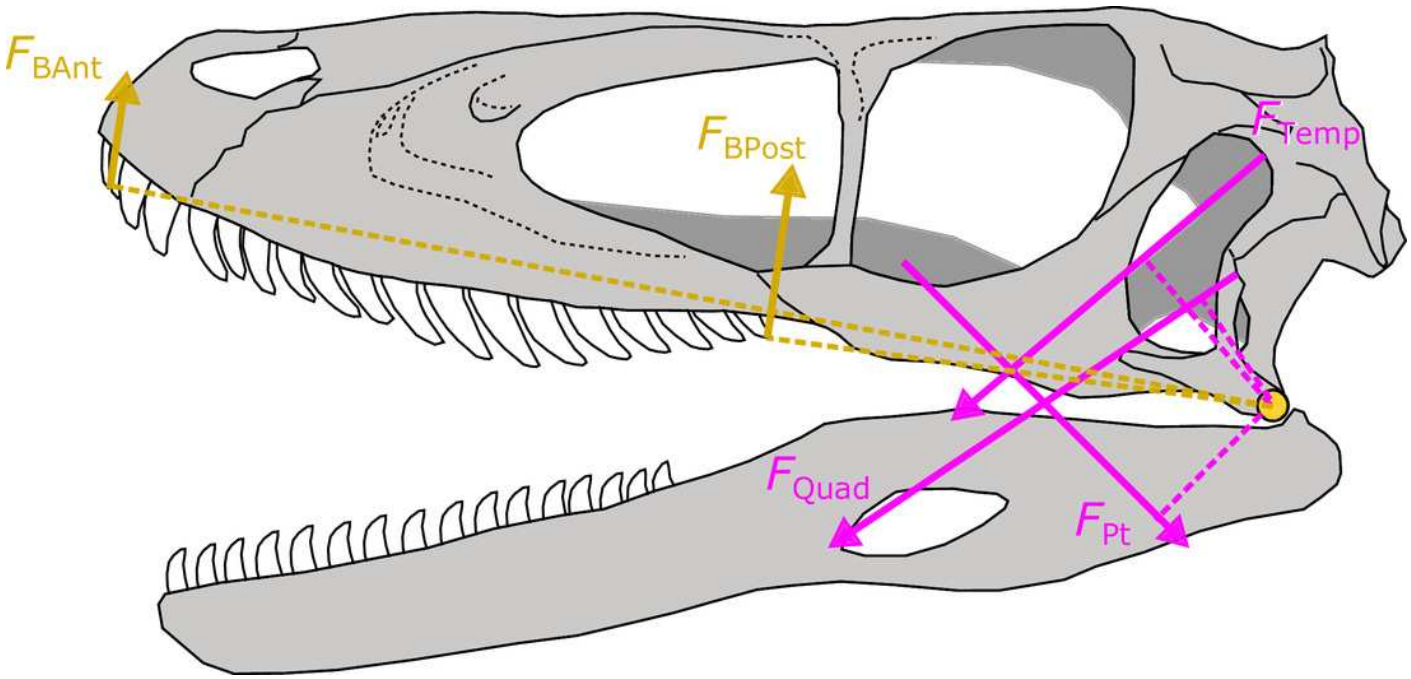

Figure 5

Relationship between bite force and skull width.

The relationship between bite force and skull width is shown for estimates based on predicted A_{Phys} (light green) and those based on muscle reconstructions (pink).

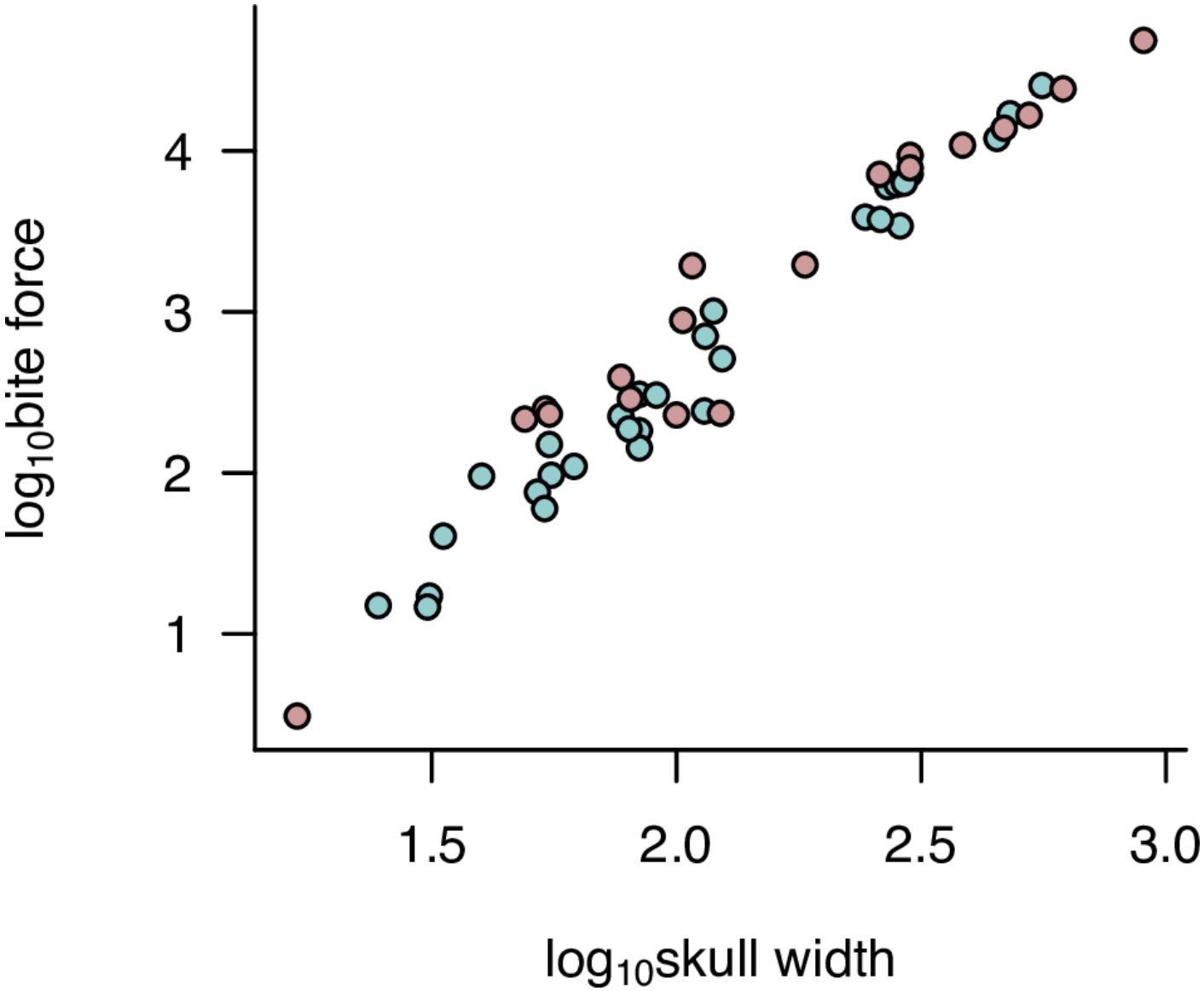

Table 1(on next page)

Bite forces estimated in extinct dinosaurs using A_{Phys} values either predicted through the PPMs or from reconstructed muscles.

F_{BAnt}, anterior bite force; F_{BPost}, posterior bite force; W_{Sk}, skull width; and A_{Phys}, physiological cross-sectional area.

Table 1. Bite forces estimated in extinct dinosaurs using A_{Phys} values either predicted through the PPMs or from reconstructed muscles. F_{BAnt}, anterior bite force; F_{BPost}, posterior bite force; W_{Sk}, skull width; and A_{Phys}, physiological cross-sectional area.

Taxon	F_{BAnt}	F_{BPost}	W_{Sk}	A_{Phys}
Acrocanthosaurus atokensis	8266	16984	480	Predicted
Bambiraptor feinbergorum	50	97	55.5	Predicted
Baryonyx walkeri	1382	3416	286	Predicted
Carcharodontosaurus saharicus	11312	25449	558	Predicted
Carnotaurus sastrei	3392	7172	300	Predicted
Ceratosaurus nasicornis	2432	5998	270	Predicted
Citipati osmolskae	202	225	77	Predicted
Compsognathus longipes	8	15	24.6	Predicted
Confuciusornis sanctus	12	17	31.3	Predicted
Deinonychus antirrhopus	298	706	114.5	Predicted
Dilong paradoxus	64	110	61.8	Predicted
Eoraptor lunensis	35	95	40	Predicted
Gallimimus bullatus	152	243	114	Predicted
Garudimimus brevipes	121	183	84	Predicted
Guanlong wucaii	268	512	124	Predicted
Haplocheirus sollers	46	76	52	Predicted
Incisivosaurus gauthieri	26	41	33.4	Predicted
Monolophosaurus jiangi	1710	3872	243	Predicted
Nanotyrannus lancensis	2068	3752	261	Predicted
Nemegtomaia barsboldi	236	308	84	Predicted
Ornithomimus edmontonicus	94	143	84	Predicted
Shuvuuia deserti	12	15	31	Predicted
Sinornithosaurus millenii	30	60	53.8	Predicted
Spinosaurus aegyptiacus	4829	11936	451	Predicted
Struthiomimus altus	108	187	80	Predicted
Teratophoneus curriei	2812	6188	282	Predicted
Tsaagan mangas	63	150	55	Predicted
Velociraptor mongoliensis	131	304	91	Predicted
Yangchuanosaurus shangyouensis	3212	6312	292	Predicted
Zupaysaurus rougieri	325	1012	119	Predicted
Allosaurus fragilis	4440	9389	300	Reconstructed
Archaeopteryx lithographica	2	3	16.8	Reconstructed
Coelophysis bauri	72	289	268	Reconstructed
Coelophysis rhodesiensis	99	393	209.2	Reconstructed

Daspletosaurus torosus	8385	16641	525	Reconstructed
Dromaeosaurus albertensis	443	885	103	Reconstructed
Erlikosaurus andrewsi	118	229	100	Reconstructed
Euparkeria capensis	86	216	49	Reconstructed
Gorgosaurus libratus	6418	13817	467	Reconstructed
Herrerasaurus ischigualastensis	678	1937	107.7	Reconstructed
Lesothosaurus diagnosticus	99	250	54	Reconstructed
Majungasaurus crenatissimus	3140	7845	300	Reconstructed
Ornithosuchus woodwardi	2910	7146	260	Reconstructed
Parasuchus hislopi	450	1958	183	Reconstructed
Plateosaurus engelhardti	82	235	123	Reconstructed
Riojasuchus tenuisceps	109	232	55	Reconstructed
Sinraptor dongi	5064	10845	384	Reconstructed
Tarbosaurus bataar	13298	24253	616	Reconstructed
Tyrannosaurus rex	25418	48505	900	Reconstructed

4